AGU PUBLICATIONS

JGR

Journal of Geophysical Research: Oceans

RESEARCH ARTICLE

10.1002/2013JC009596

Special Section:

Early scientific results from the salinity measuring satellites Aquarius/SAC-D and SMOS

Key Points:

- Ocean eddy freshwater flux is significant marine hydrological budget component
- Mesoscale salinity features are prevalent in the NA subtropical surface layer
- >50% of air-sea water vapor flux from NA subtropics is balanced by eddies

Correspondence to:

A. L. Gordon,
agordon@ldeo.columbia.edu

Citation:

Gordon, A. L., and C. F. Giulivi (2014), Ocean eddy freshwater flux convergence into the North Atlantic subtropics, *J. Geophys. Res. Oceans*, *119*, doi:10.1002/2013JC009596.

Received 8 NOV 2013
Accepted 12 MAY 2014
Accepted article online 17 MAY 2014

Ocean eddy freshwater flux convergence into the North Atlantic subtropics

Arnold L. Gordon[1] and Claudia F. Giulivi[1]

[1]Lamont-Doherty Earth Observatory of Columbia University, Palisades New York, USA

Abstract For a quasi steady state condition, the water vapor flux from the ocean to atmosphere typical of the salty subtropics must be compensated by ocean processes that transfer freshwater into the evaporative regime. Observations of the North Atlantic subtropical sea surface salinity maximum region frequently reveal the presence of eddies with distinct salinity/temperature signatures of up to 0.2 psu/1°C, with horizontal scales of up to 200 km. Using the surface layer salinity and meridional velocity from the Simple Ocean Data Assimilation (SODA) reanalysis data, we find that the eddy flux can accomplish 50% to 75% of the required freshwater convergence into the subtropical regime, the rest being delivered by Ekman transport convergence, and therefore represents a significant component of the marine hydrological cycle. Interannual fluctuations of the eddy freshwater flux are reflected in sea surface salinity variability.

1. Introduction

The more often and better we observe the ocean, with improved instrumentation and models, the less it looks like the familiar "climate" field of overly smoothed fields of sea surface temperature and salinity (SST, SSS), and more of a highly textured pattern of O(100 km) and finer horizontal scales (Figure 1a). This is particularly true of the saline subtropical regimes, where sea surface height anomalies revealed by satellite altimeter [*Chelton et al*., 2011] reflect the ocean eddy field, which may be considered as the "weather of the ocean."

The North Atlantic subtropics (Figure 1) exhibit sea surface salinity (SSS) of greater than 37.0 practical salinity units (psu), with a SSS-max residing near the 24°–25°N, making it the saltiest of the oceanic subtropical regimes. The mean geostrophic surface flow is directed toward the south, marking the eastern limb of the subtropical gyre. The trade wind induced Ekman transport south of the SSS-max is directed toward the north, forming the upper limb of the ocean shallow meridional circulation cell [*Worthington*, 1976; *Talley*, 2008]. North of the SSS-max to 40°N the Ekman transport is weak. The resultant Ekman convergence of relatively low salinity surface water into the SSS-max regime is the traditional explanation for the ocean process that compensates the net water vapor loss to the atmosphere, by excess evaporation (E) over precipitation (P) (Figure 2).

While the gradient of the meridional Ekman transport with latitude across the North Atlantic subtropical region is nearly linear, the meridional gradient of the sea surface density is greater to the south of the SSS-max, in the 10°–25°N band (Figure 3), as the more buoyant, warm, low SSS tropical water, "presses" into the cooler, saltier subtropical region of reduced northward Ekman transport. The meridional gradient of density ($d\rho/dy$) projects below the Ekman layer by the induced downward vertical velocity at the base of this layer (Ekman pumping). The large $d\rho/dy$ of the surface layer coincides with the maximum of eddy kinetic energy as revealed by satellite altimeter [*Fratantoni*, 2001] and simulated in models, reaching a seasonal maximum in late spring (Busecke et al., 2014, Mesoscale turbulence within the subtropical North Atlantic surface layer, submitted to *Journal of Geographical Research: Oceans*), which may be an important pathway of providing low SSS into the evaporative subtropics via eddy processes, as discussed below. The relatively strong meridional gradient of sea surface density in the interval 15°–20°N generated by the Ekman transport, may induce baroclinic instability and eddy generation [*Gill et al*., 1974; *Gill*, 1982]. *Cessi* [2007] noted that Ekman pumping can introduce available potential energy on which eddies can grow. In this way, the Ekman transport and eddy field are not independent.

The focus of this study is to evaluate the premise that Reynolds fluxes (u'S'), associated with ocean eddies is a significant factor in compensating for the North Atlantic subtropical sea to air water vapor flux, and is an essential part of the marine hydrological cycle. Using Simple Ocean Data Assimilation reanalysis data [SODA; *Carton and Giese*, 2008], we focus on the >100 km eddy field. The complex patterns of smaller sub-mesoscale features and their role in freshwater fluxes, investigated as part of the Salinity Processes in the

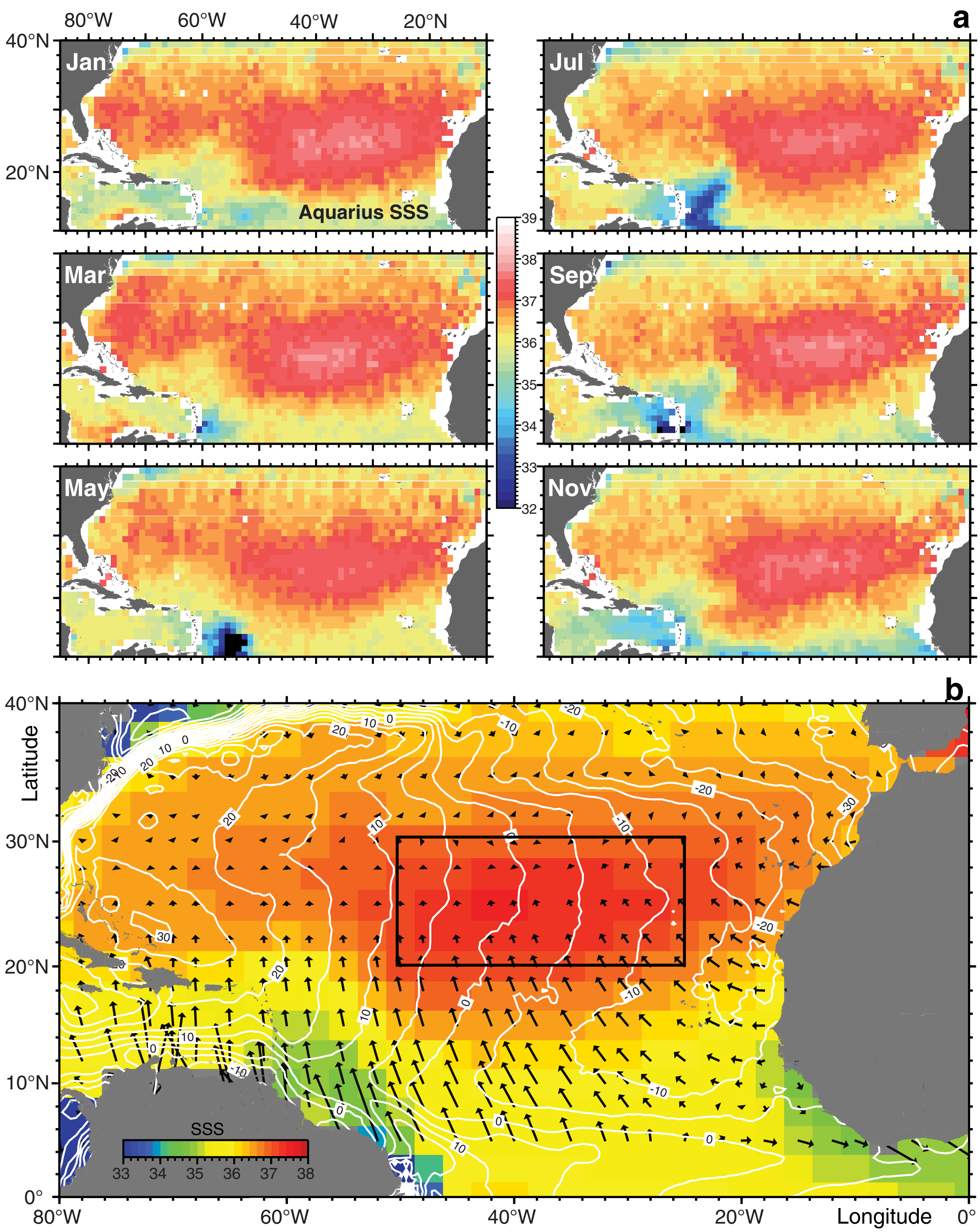

Figure 1. North Atlantic subtropical sea surface salinity. (a) Sea surface salinity (SSS) for January-November 2012 (every other month) from Aquarius Version 2.0 Level-3 monthly binned data (http://podaac.jpl.nasa.gov). (b) Climatological annual mean SSS (upper 20 m average), computed from the 1° × 1° World Ocean Atlas [WOA09; *Antonov et al.*, 2010]. The Ekman transport vectors in Sverdrups (1 Sv = 10^6 m^3/s) were calculated within a 2.5° × 2.5° cell using long-term mean wind stresses based on ECMWF (European Center for Medium Range Weather Forecasting) 40 year reanalysis (ERA-40) monthly reanalysis data [*Uppala et al.*, 2005]. Contours of mean ocean dynamic topography (MDOT) calculated from analyzed data from near-surface drifters, satellite altimetry, NCEP wind, and the GRACE geoid model for the decade 1992–2002 [*Maximenko et al.*, 2009; http://apdrc.soest.hawaii.edu/projects/DOT/]. The box indicates the subtropical region (20°–30°N; 50°–25°W) considered in this study. All SSS data are displayed in practical salinity units (psu).

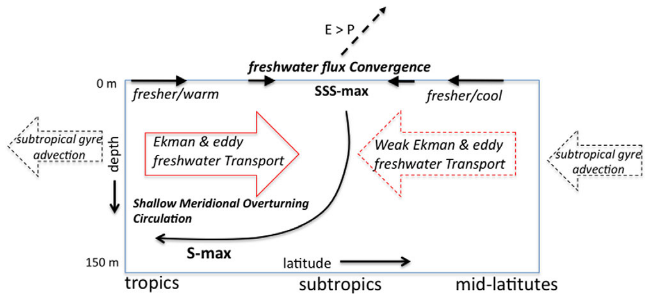

Figure 2. Schematic of the meridional freshwater balance within the ocean subtropical regime. Net evaporation associated with the poleward edge of the atmospheric Hadley Cell is compensated by convergence of freshwater by ocean processes. These include Ekman convergence and eddy fluxes, in addition to the large-scale ocean advection from the north as part of the subtropical gyre. Subtropical surface layer is removed by sinking and spreading toward the tropics as part of the shallow meridional overturning circulation.

Upper Ocean Regional Study (SPURS) in the North Atlantic, are discussed by Busecke et al. (submitted manuscript, 2014).

2. North Atlantic Subtropical Sea Surface Salinity

Monthly SSS fields from Aquarius satellite data [*Lagerloef et al*., 2008, 2012; Figure 1a] for 2012 reveal a seasonal monthly shift in the position and amplitude of the SSS-max pattern, reaching the maximum areal extent in the January-March period with a northward displacement and contraction from July to December (also see Bingham et al., 2014, The North Atlantic sea surface salinity maximum as observed by Aquarius, submitted to *Journal of Geophysical Research: Oceans*). The long-term mean monthly values derived from the in situ ocean surface observations from Ships Of Opportunity Program [SOOP; *Delcroix et al*., 2005; *Reverdin et al*., 2007; Figure 4] are consistent with the 2012 Aquarius SSS-max shifts. The SOOP-derived data show that the SSS-max, within the latitude range of 20°–30°N and longitude range of 50°W–25°W (the black box shown in Figure 1 referred to as the "subtropical box") shifts northward by over 1° of latitude and increases in salinity by 0.2 psu from April to September. The seasonal range of SSS is markedly higher to the north of the SSS-max.

The seasonal progression of the average SSS within the subtropical box (Figure 4d) has the SSS minimum in March with a maximum in October. While E-P is always positive, it is greater in winter, with a secondary July peak, and minimum in September-October, the SSS cycle is out-of-phase, with a maximum in October, and a minimum in April. If the SSS were solely a function of E-P, the SSS would increase continuously, but at a lesser rate in the summer/fall transition. Lower winter/spring SSS is presumed a consequence of greater freshwater flux during winter, perhaps a result of fall and winter deepening mixed layer [*Kara et al*., 2003; *de Boyer Montegut et al*., 2004], entraining lower salinity thermocline water and/or due to seasonality of the horizontal eddy freshwater flux.

3. Data and Methods

To assess the hypothesis that flux of freshwater by eddies plays a significant role in providing for a quasi steady state condition, we first use the salinity and meridional velocity data from a synoptic zonal section across the North Atlantic subtropical box obtained by the RAPID program (http://www.rapid.ac.uk/rapidmoc/) (Figures 5a–5c), specifically the Conductivity-Temperature-Depth (CTD) profiles and observations of currents in the upper 500 m collected by the RRS Discovery Cruise D279 section along 24.5°N during April-May 2004 [*Cunningham*, 2005]. The RAPID D279 section provides an estimate of the eddy fluxes across a latitude within the subtropical box at a specific time.

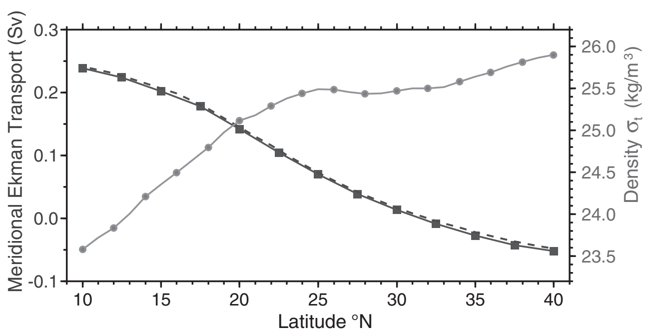

Figure 3. Ekman dynamics. Average meridional Ekman transport (Sv) across 1° of longitude within the North Atlantic subtropical region (50°–25°W) computed from the meridional components of the Ekman transports shown in Figure 1b using ERA-40 (squares) and SODA (dash) wind stress values. The gray line shows the sea surface density, from surface salinity and temperature values from the annual WOA09 data [*Antonov et al*., 2010; *Locarnini et al*., 2010], zonally averaged over the same longitudes.

To achieve a broader temporal and spatial view of the eddy flux at scales >100 km, we use salinity and meridional velocity data from SODA

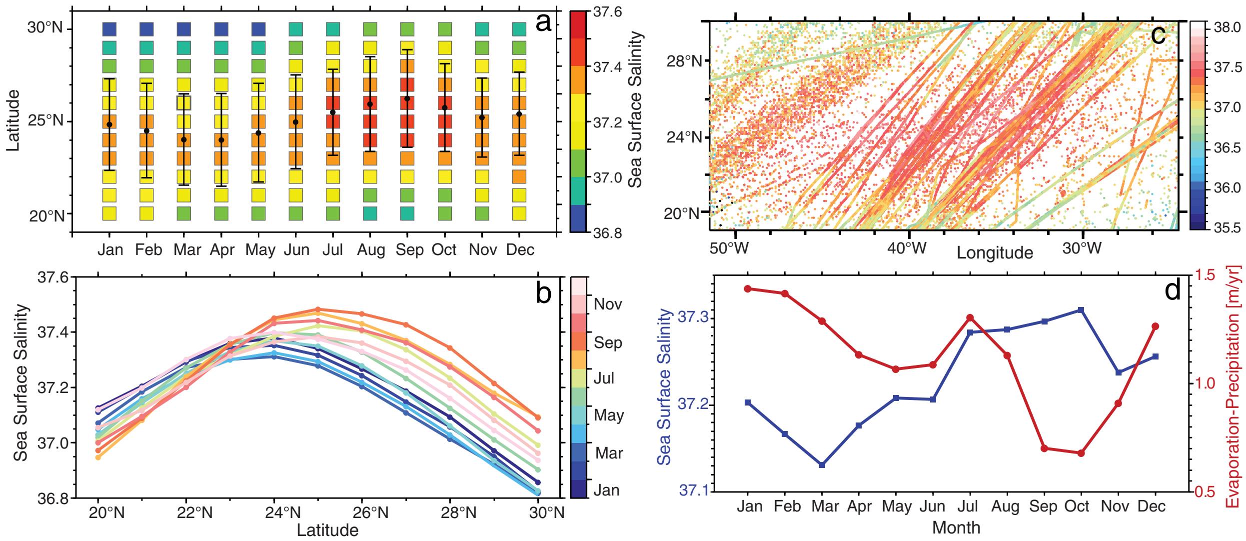

Figure 4. Variability of the SSS maximum. (a) Monthly SSS climatology from gridded 1° × 1° data within the region shown by the box in Figure 1b, as a function of latitude [*Reverdin et al.*, 2007; http://www.legos.obs-mip.fr/observations/sss/datadelivery/sea-surface-salinity-database-in-the-atlantic-ocean-50degn-30degs-for-the-1970–2002-period]. (b) As in Figure 4a but shown as a function of longitude and color coded by months. (c) Distribution of the validated SSS [*Delcroix et al.*, 2005; http://www.legos.obs-mip.fr/observations/sss] for the period 1950–2003, color-coded by salinity. The SSS is distributed along the trans-oceanic SOOP tracks. (d) Monthly salinity (upper 20 m; blue) from the WOA09 [*Antonov et al.*, 2010] and evaporation minus precipitation (red; m/yr) from ERA-40, for the same box as a function of month.

extending the analysis to other months, and eventually to other years and to other latitudes of the subtropical box. We use SODA reanalysis data version 2.2.4 for the period 1970–2010 (monthly data are available from http://soda.tamu.edu/assim/). The ocean model is based on Parallel Ocean Program (POP) physics with a horizontal resolution of 0.4° longitude × 0.25° latitude and with 40 levels on the vertical, with 10 m spacing near the surface. Output variables are monthly averaged and mapped onto a uniform global 0.5° × 0.5° × 40 levels grid, which at 25°N is 55 km in the north-south direction and 50 km in the east-west direction [*Carton et al.,* 2005; *Carton and Giese*, 2008; *Giese and Ray*, 2011]. Observations assimilated into SODA include all available hydrographic profile data, as well as ocean station data, moored time series, surface temperature, and salinity observations of various types from the World Ocean Database 2009 [*Boyer et al.*, 2009]; surface temperature data are from ICOADS 2.5 [*Woodruff et al.*, 2011] and surface boundary conditions for momentum and heat and salt fluxes are derived from the 20CRv2 reanalysis [*Compo et al.*, 2011].

Mesoscale features shift westward across the North Atlantic subtropical box at a rate of ~4 km/day [*Fu and Chelton*, 2001; *Chelton et al.*, 2011]. The RAPID section takes 11 days to span the 25°–50°W interval and so captures the eddies. The monthly SODA reanalysis "data" provide a gridded smoothed product, relative to synoptic sections, and therefore would underestimate the eddy flux. Additionally, the SODA resolution will represent the eddy field >100 km, the lower frequency end of the mesoscale activity. The results of the SPURS field program, and higher resolution models, capture the higher frequency behavior (Busecke et al., submitted manuscript, 2014).

To evaluate the SODA representation of the eddy freshwater (FW) flux across the latitudes of the subtropical box, we first compare the SODA eddy flux to the FW flux derived from the RAPID section across 24.5°N (Figure 5). We then use the SODA data to calculate eddy FW flux within the other latitudes of the subtropical box to determine the freshwater convergence, and compare to E-P data estimates, for all months of 2004. We also examine interannual changes of the FW flux extending the same analysis for the SODA time span of 1970–2010.

The meridional eddy freshwater flux in m^3/s is calculated as follows: the product of the salinity anomaly and the meridional velocity anomaly at 5 m depth across the longitude range of the subtropical box (Figure 1) is determined. The anomaly values are the value at specific longitude, or grid point, relative to the section mean salinity and meridional velocity. We assume that the 5 m (for a meter thick layer) FW flux represents

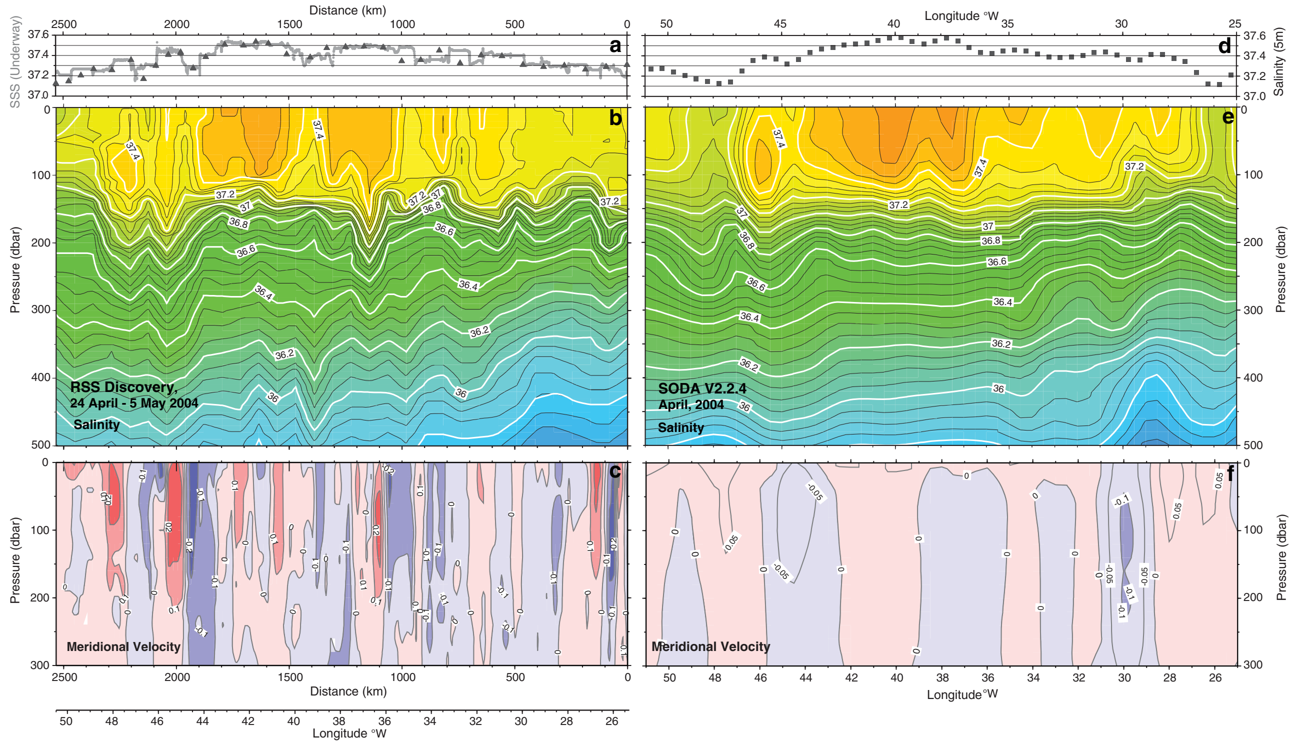

Figure 5. Salinity and meridional velocity sections along ~ 24.5°N. The sections are displayed against pressure (dbar) in the vertical and distance (km) and longitude (°W) in the horizontal. Left plots from data collected by the RRS Discovery RAPID Cruise D279 from 24 April to 5 May 2004 [*Cunningham*, 2005]; right plots are constructed from April 2004 SODA ocean reanalysis Version 2.2.4 data. (a) RAPID Cruise D279 SSS data from the TSG system (gray line); the symbols (black) represent an average of the upper 10 m salinity data from the vertical conductivity-temperature-depth (CTD) profiles. (b) RAPID Cruise D279 vertical salinity section from CTD data. (c) Meridional velocity measured by the underway hull mounted acoustic Doppler current profiler (ADCP) system. Blue are southward-directed currents; red are northward-directed currents. (d-f) As the left plots, but for the April 2004 monthly SODA data.

the FW flux within the mixed layer. Summarizing at each latitude, from 20°N to 30°N we estimate the fluxes as:

$$\sum s_i' v_i'$$

where, the salinity anomalies are defined as $s'=1-s_i/s$; i represents each longitude from 25°W to 50°W; s is the mean SSS along that section and s_i is the salinity at a specific longitude; in the same way, the meridional velocity anomalies v' are defined as $v'=v_i-v$. Both salinities and velocities were taken from the first level of SODA data (5 m) and represent the upper 10 m.

The September/October 2012 SPURS cruise data collected in the North Atlantic subtropical box show a mean mixed layer of 50 m, whereas the mixed layer in March/April 2013 was 100 m (R. Schmitt, personal communication, 2013). This is consistent with the mixed layer seasonal behavior reported by *de Boyer Montegut et al*. [2004], who estimate the monthly mixed layer depth within the North Atlantic subtropical regime as varying from a winter value of approximately 100 m, decreasing to typical spring/summer values of 50 m, returning to 100 m during the autumn months. These mixed layer values are also in agreement with those derived from Argo profilers and reported at the Japan Agency for Marine-Earth Science and Technology (JAMSTEC) database (http://www.jamstec.go.jp/ARGO/argo_web/prod/mila_monthly_e.html) and with values from the Argo gridded products at the Asia Pacific Research Center (APDRC; http://apdrc.soest.hawaii.edu/projects/Argo/). Busecke et al. (submitted manuscript, 2014) note that freshwater anomalies to the south of the SSS-max extend down to 50–80 m. Here, we use 50 meters, the seasonal minimum of the mixed layer, one that encompassed the low salinity surface layer features observed by SPURS, to estimate the freshwater flux; we then consider the effect of the deeper winter mixed layer.

It is not the freshwater flux across specific latitudes, but rather the meridional eddy freshwater flux convergence (negative divergence), which compensates for net E-P water vapor flux. Rather than differencing the

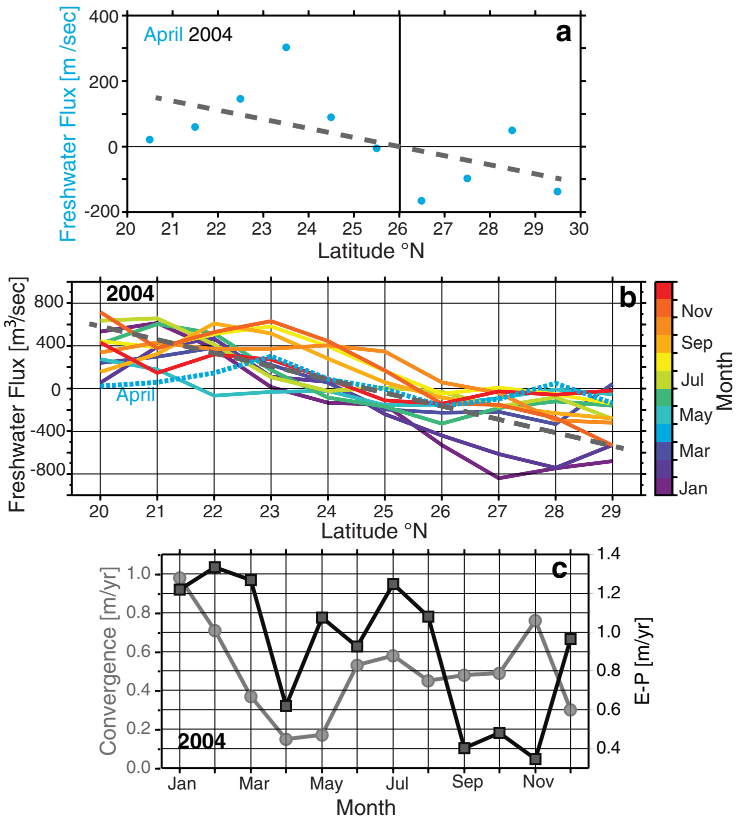

Figure 6. Meridional eddy freshwater fluxes for 2004 SODA data. (a) Freshwater flux against latitude for April 2004. Calculations were made for 1° latitude bands between 50°W and 25°W, and using the 5 m SODA salinity and meridional velocity values, applied to a 50 m surface layer slab. The SODA data are available at 0.5° × 0.5° lat/long. (b) Monthly distribution of the freshwater flux for 2004; the dashed line is a linear fit to the monthly freshwater flux values. (c) Freshwater convergence (m/yr) for 2004 for the entire box plotted against months (left axis; gray). E-P (m/yr; right axis) with evaporation from the WHOI OAFlux project (http://oaflux.whoi.edu) and precipitation from the Global Precipitation Climatology Project (GPCP) V2.2 (https://climatedataguide.ucar.edu/climate-data/gpcp-monthly-global-precipitation-climatology-project.).

meridional FW flux across 20° and 30°N, the latitude limits of the subtropical box (Figure 1b), the FW convergence is determined from the slope of a linear fit to the eddy freshwater fluxes at each latitude of the subtropical box, dFW/dy, to provide a more robust estimate. The FW flux across 25°W and 50°W longitude boundaries are relatively small. The net accumulation of freshwater within the subtropical box is given in meter per second.

4. Results

Inspection of the RAPID salinity and meridional velocity sections (Figures 5a and 5b) and temperature sections (not shown), as well as of Aquarius SSS maps and ship-based ThermoSalinoGraph (TSG) data reveal a pronounced mesoscale field with coherent surface and subsurface temperature and salinity signals. The TSG data collected during the April 2004 transect display sharp salinity fronts with significant correlation ($>$ 0.85) with the upper 20 m salinity derived from CTD data (Figure 5a). The hydrographic sections show distinct alternating low-high salinity banding associated with meridional reversal velocities (Figure 5b) of horizontal scales O(100) km. Vertical profiles (not shown) show a uniform surface layer that extends down to ~50 m, in agreement with climatology. The SODA section (Figures 5d–5f) reproduces these features, albeit with a smoother velocity field (Figure 5f), capturing, as discussed above, the lower frequency end of the eddy pattern.

The Reynolds freshwater flux across the RAPID section taken from 24 April to 5 May at 24.5°N between 25°W and 50°W and for a 50 m thick mixed layer is +310 m^3/s. The SODA reanalysis data for April 2004

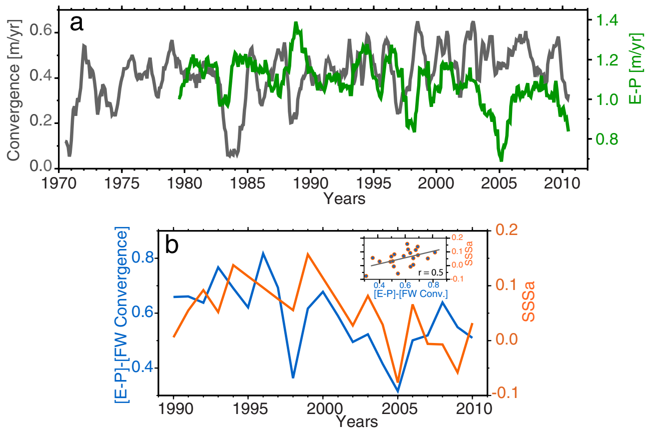

Figure 7. Variability of the freshwater convergence, evaporation minus precipitation, and SSS variability. (a) 12-month running mean freshwater convergence (gray line; m/yr), into the subtropical box (Figure 1b) for 1970–2010 SODA data and E-P (green), calculated from WHOI OAFlux E and GPCP P. (b) Annual FW convergence and E-P difference (blue) and SSS anomalies (SSSa; orange) for the subtropical gyre box for 1990–2010. The SSSa, based on WOAD09 data [*Boyer et al.*, 2009], is the anomaly relative to the mean SSS calculated with 2° boxes within the SSS-max region, defined as SSS higher than 37.2 psu. Also shown, the scatter plot between these time series.

yield a freshwater flux across 24°–25°N of +100 m^3/s (Figure 6a), about 1/3 of that determined from the RAPID data. The reduced flux is likely due to the averaging of the SODA data across larger spatial and temporal domain.

Applying the same methods to the April 2004 SODA data and to the rest of the latitudes of the subtropical box, we can determine the slope of the linear fit to the derived freshwater fluxes versus latitude. This value yields a convergence of freshwater of 0.15 m/yr, annualized from the April 2004 value, representing the freshwater accumulation spread uniformly over the subtropical box. This is repeated for each month (Figure 6b) to derive the 2004 annual values of freshwater convergence (Figure 6c).

We find that the freshwater convergence varies from a low of 0.15 m/yr in April and May 2004 to a maximum in January, February, and November 2004, of greater than 0.70 m/yr. The yearly average is 0.5 m/yr. This would compensate approximately 50% of the annual E-P of 1.1 m/yr estimated for the same region [*Schanze et al.*, 2010]. As the SODA data are expected to underestimate the freshwater flux by the mesoscale, the FW eddy flux is expected to be larger. Eddy flux of freshwater into the evaporative subtropical North Atlantic represents a significant source of freshwater as required for the maintenance of a steady state SSS-max.

We used a constant 50 m surface layer slab, as it is the minimum value for the seasonal mixed layer, and includes the layer with the largest low salinity features (Busecke, et al., submitted manuscript, 2014). Using an annual average mixed layer with a range of approximately 100 m for the winter months to decreasing values of 50 m for the spring/summer months [*de Boyer Montegut et al.*, 2004], would increase the annual FW convergence to ~75% of the annual net E-P loss of freshwater.

For comparison, we use the SODA data to estimate the effective E-P to balance the net Ekman convergence. The Ekman transport across 1 meter wide strip at 20°N is 1.450 m^3/s; across 30°N it is 0.170 m^3/s. The SODA salinity at 5 m for each latitude is, 37.1 and 36.8, respectively. The SODA subsurface S-max emanating from the SPURS area is 37.45, in agreement with the Argo climatology shown by Busecke et al. (submitted manuscript, their Figure 4, 2014). A simple calculation finds an E-P of 0.30 m/yr is needed to balance the Ekman transport convergence. This value with the eddy FW convergence sum to around 1 m/yr (using seasonally variable mixed layer thickness) which is close to the estimated annual E-P of 1.1 m/yr, with the eddy term providing 2/3 of the required fluxes for a quasi stationary salinity pattern.

The eddy freshwater convergence (Figure 7a) for the period covered by the SODA reanalysis, 1970–2010, reveals interannual variability, from a low of $<$ 0.1 m/yr in 1970 and in 1983, 0.2 m/yr in 1988 and 0.25 m/yr in 1996/97; to a high of 0.6 m/yr in 1998 and in 2002, though this result is far from robust, it is included here only to indicate that interannual variability of eddy FW flux is a factor, in addition to E-P, in driving SSS-max year to year fluctuations. In the western North Atlantic subtropics, the SSS fluctuations respond to ENSO and PDO (El Niño Southern Oscillation, and Pacific Decadal Oscillation, respectively) [*Gordon and Giulivi*, 2008], which may extend to the subtropical box considered in this study [see Figure 6 of *Gordon and Giulivi*, 2008]. Interannual changes in the SSS-max depend on many factors such as E-P and advection and mixing processes, including Ekman transport variability and lateral and vertical turbulence. The monthly cycle of FW flux does not show a marked seasonal cycle (not shown) suggesting that the SSS annual cycle may be a product of seasonal deepening of the mixed layer rather than increased eddy activity.

Plotting the annual differences of E-P and eddy freshwater convergence (Figure 7b) against the SSS anomalies within the SPURS area reveal an expected relationship, albeit weak, with SSS decreasing when E-P is small relative to the eddy freshwater convergence.

5. Conclusions

We provide evidence based on SODA reanalysis data that eddy flux of freshwater into the evaporative subtropics of the North Atlantic is likely a major factor in compensating for the net E-P. Freshwater convergence by ocean eddies is an essential part of the marine hydrological cycle, shaping the sea surface salinity spatial and temporal pattern. We can fine-tune the SODA analysis to the monthly mixed layer, but that is best left for higher resolution model output and views of the regional salinity fields as evolving from satellite and Argo data sets.

Satellite-based observations of sea surface salinity (from Aquarius and SMOS missions) with geostrophic surface current calculated from sea surface height data from satellite altimeter, as well as a more complete view of the seasonal and possible interannual fluctuations of the mixed layer depth within the subtropical box of the North Atlantic, as afforded by Argo profilers, will enable a more quantitative evaluation quantify freshwater convergence by mesoscale eddies on the near global ocean scale. HYCOM model output will provide high-spatial/temporal resolution-based estimates.

Acknowledgements
NASA grant number NNX09AU68G provided support for this research. We thank Stuart Cunningham for providing the RAPID data. We appreciate the constructive comments from Zhijin Li, Frederick Bingham, and Julius Busecke. Lamont-Doherty Earth Observatory contribution number 7794.

References

Antonov, J. I., D. Seidov, T. P. Boyer, R. A. Locarnini, A. V. Mishonov, H. E. Garcia, O. K. Baranova, M. M. Zweng, and D. R. Johnson (2010), *World Ocean Atlas 2009, Volume 2: Salinity*, edited by S. Levitus, 184 pp., *NOAA Atlas NESDIS 69*, U.S. Gov. Print. Off., Washington, D. C.

Boyer, T. P., et al. (2009), *World Ocean Database 2009*, edited by S. Levitus, 206 pp., *NOAA Atlas NESDIS 66*, U.S. Gov. Print. Off., Washington, D. C., DVDs.

Carton, J. A., and B. S. Giese (2008), A reanalysis of ocean climate using Simple Ocean Data Assimilation (SODA), *Mon. Weather Rev.*, *136*, 2999–3017.

Carton, J. A., B. S. Giese, and S. A. Grodsky (2005), Sea level rise and the warming of the oceans in the Simple Ocean Data Assimilation (SODA) ocean reanalysis, *J. Geophys. Res.*, *110*, C09006, doi:10.1029/2004JC002817.

Cessi, P. (2007), Regimes of thermocline scaling: The interaction of wind stress and surface buoyancy, *J. Phys. Oceanogr.*, *37*, 2009–2021.

Chelton, D. B., M. G. Schlax, and R. M. Samelson (2011), Global observations of nonlinear mesoscale eddies, *Prog. Oceanogr.*, *91*, 167–216.

Compo, G. P., et al. (2011), The Twentieth Century Reanalysis Project. *Q. J. R. Meteorol. Soc.*, *137*, 1–28, doi:10.1002/qj.776.

Cunningham, S. A. (2005), *RRS Discovery Cruise 279 (04 Apr10–May 2004): A Transatlantic Hydrography Section at 24.5° N.*, Cruise Report 54, 1–199, Southampton Oceanography Centre. [Available at http://eprints.soton.ac.uk/17527/.]

de Boyer Montégut, C., G. Madec, A. S. Fischer, A. Lazar, and D. Iudicone (2004), Mixed layer depth over the global ocean: An examination of profile data and a profile-based climatology, *J. Geophys. Res.*, *109*, C12003, doi:10.1029/2004JC002378.

Delcroix, T., A. Dessier, Y. Gouriou, and M. McPhaden (2005), Time and space scales for sea surface salinity in the tropical oceans, *Deep Sea Res., Part I*, *52*, 787–813.

Fratantoni, D. M. (2001), North Atlantic surface circulation during the 1990's observed with satellite-tracked drifters, *J. Geophys. Res.*, *106*, (C10), 22067–22093.

Fu, L.-L. and D. B. Chelton (2001), Large-scale ocean circulation, in *Satellite Altimetry and the Earth Sciences: A Handbook of Techniques and Applications*, edited by L.-L. Fu, A. Cazenave, pp. 133–169, Academic Press, San Diego, Calif.

Gill, A. (1982), *Atmosphere-Ocean Dynamics, Int. Geophys. Ser.*, vol. 30, 662 pp., Academic Press, N. Y.

Gill, A. E., J. S. A. Green, and A. J. Simmons (1974). Energy partition in the large-scale ocean circulation and the production of mid-ocean eddies, *Deep Sea Res., 21*, 499–528.

Gordon, A. L. and C. F. Giulivi (2008), Sea surface salinity trends over 50 years within the Subtropical North Atlantic, *Oceanography*, *21*, 20–29.

Giese B. S. and S. Ray (2011), El Nino variability in simple ocean data assimilation (SODA), 1871–2008, *J. Geophys. Res*, *116*, C02024, doi: 10.1029/2010JC006695.

Kara, A. B., P. A. Rochford, and H. E. Hurlburt (2003), Mixed layer depth variability over the global ocean, *J. Geophys. Res.*, *108*(C3), 3079, doi: 10.1029/2000JC000736.

Lagerloef, G., et al. (2008), The Aquarius/SAC-D Mission: Designed to meet the salinity remote-sensing challenge. *Oceanography*, *21*, 68–81.

Lagerloef, G., F. Wentz, S. Yueh, H. Y. Kao, G. C. Johnson, and J. M. Lyman (2012), Aquarius satellite mission provides new, detailed view of sea surface salinity, State of the Climate in 2011, *Bull. Am. Meteorol. Soc.*, *93*, 7, S70–S71.

Locarnini, R. A., A. V. Mishonov, J. I. Antonov, T. P. Boyer, H. E. Garcia, O. K. Baranova, M. M. Zweng, and D. R. Johnson (2010), *World Ocean Atlas 2009, Volume 1: Temperature*, edited by S. Levitus, 184 pp., *NOAA Atlas NESDIS 68*, U.S. Gov. Print. Off., Washington, D. C.

Maximenko, N., P. Niiler, M.-H. Rio, O. Melnichenko, L. Centurioni, D. Chambers, V. Zlotnicki, and B. Galperin (2009), Mean dynamic topography of the ocean derived from satellite and drifting buoy data using three different techniques. *J. Atmos. Oceanic Technol.*, *26*(9), 1910–1919.

Reverdin, G., E. Kestenare, C. Frankignoul, and T. Delcroix (2007), Surface salinity in the Atlantic Ocean (30S-50N), *Prog. Oceanogr.*, *73*, 311–340.

Schanze, J. J., R. W. Schmitt, and L. L. Yu (2010), The global oceanic freshwater cycle: A state of the art quantification, *J. Mar. Res.*, *68*(3-4), 569–575.
Talley, L. D. (2008), Freshwater transport estimates and the global overturning circulation: Shallow, deep and throughflow components, *Prog. Oceanogr.*, *78*, 257–303.
Uppala, S. M., et al. (2005), The ERA-40 re-analysis, *Q. J. R. Meteorol. Soc.*, *131*, 2961–3012.
Woodruff, S. D., et al. (2011), ICOADS Release 2.5: Extensions and enhancements to the surface marine meteorological archive, *Int. J. Climatol.*, *31*, 951–967.
Worthington, L. V. (1976), The formation of salinity-maximum water, *Johns Hopkins Oceanogr. Stud.*, *6*, 85–91.

